RADIATION RESEARCH **186**, 189–195 (2016)
0033-7587/16 $15.00

DOI: 10.1667/RR14431.1

Radiation-Induced Microvascular Injury as a Mechanism of Salivary Gland Hypofunction and Potential Target for Radioprotectors

Aviram Mizrachi,[a] Ana P. Cotrim,[d] Nora Katabi,[b] James B. Mitchell,[d] Marcel Verheij[e] and Adriana Haimovitz-Friedman[c,1]

Departments of [a] Surgery, Head and Neck Service, [b] Pathology and [c] Radiation Oncology, Memorial Sloan-Kettering Cancer Center, New York, New York; [d] Radiation Biology Branch, National Cancer Institute, National Institute of Health, Bethesda, Maryland; and [e] Department of Radiation Oncology, Netherlands Cancer Institute, Amsterdam

Mizrachi, A., Cotrim, A. P., Katabi, N., Mitchel, J. B., Verheij, M. and Haimovitz-Friedman, A. Radiation-Induced Microvascular Injury as a Mechanism of Salivary Gland Hypofunction and Potential Target for Radioprotectors. *Radiat. Res.* 186, 189–195 (2016).

Radiation therapy is commonly used to treat patients with head and neck squamous cell carcinoma (HNSCC). One of the major side effects of radiotherapy is injury to the salivary glands (SG), which is thought to be mediated by microvascular dysfunction leading to permanent xerostomia. The goal of this study was to elucidate the mechanism of radiation-induced microvasculature damage and its impact on SG function. We measured bovine aortic endothelial cell (BAEC) apoptosis and ceramide production in response to 5 Gy irradiation, either alone or with reactive oxygen species (ROS) scavengers. We then investigated the effect of a single 15 Gy radiation dose on murine SG function. BAECs exposed to 5 Gy underwent apoptosis with increased ceramide production, both prevented by ROS scavengers. Among the 15 Gy irradiated mice, there was considerable weight loss, alopecia and SG hypofunction manifested by reduced saliva production and lower lysozyme levels. All of these effects, except for the lysozyme levels, were prevented by pretreatment with ROS scavengers. Microvessel density was significantly lower in the SG of irradiated mice compared to the control group, and this effect was significantly attenuated by pretreatment with Tempol. This study demonstrates that radiation-induced SG hypofunction is to a large extent mediated by microvascular dysfunction involving ceramide and ROS generation. These findings strongly suggest that ROS scavengers may serve as potential radioprotectors of SG function in patients undergoing radiotherapy for HNSCC.

INTRODUCTION

Head and neck squamous cell carcinoma (HNSCC) is the sixth most common malignancy worldwide (*1*). The curative treatment modalities for most HNSCCs consist of surgery and/or radiation therapy. Chemotherapy is added as a radiosensitizer and to decrease the risk of developing distant metastasis in high-risk patients (*2*). One of the most severe and devastating side effects of radiation therapy is damage to major and minor salivary glands (SGs), resulting in salivary hypofunction in ~80% of patients (*3*). This may lead to permanent xerostomia, which causes considerable morbidity, including dental caries, mucosal infections and dysphagia that adversely affect patients' quality of life (*4, 5*).

Several theories have emerged aiming to provide a comprehensive explanation for the underlying mechanism of radiation-induced SG damage, which has been considered as enigmatic since first described in 1911 (*6*). One hypothesis is that radiation exposure results in sublethal DNA damage, which becomes lethal at a delayed phase. Thus, when the acinar progenitor cells are going through a reproductive phase and parenchymal replenishment is required, these cells undergo cell death (*7*). More recently, it has been found that microvascular endothelial cells within the SGs are the primary targets for radiation-induced damage (*8*). Thus, it may be possible that protecting the microvasculature prevents radiation-induced salivary hypofunction and might also enable recovery of the acinar progenitor cells from the initial insult.

Both acute and late tissue damage after irradiation have been linked to the endothelial damage in normal tissues (*9*). In a previous study, we reported that the molecular mechanisms involved in the endothelial response to radiation were associated with signaling from the plasma membrane, mainly via the acid sphingomyelinase/ceramide (ASMase/Ceramide) pathway (*10, 11*). Data from our group and others showed that a number of radiation-induced injuries to normal tissues result from damage to endothelial cells by the ASMase pathway (*12, 13*). Moreover, several

[1] Address for correspondence: Department of Radiation Oncology, Memorial Sloan-Kettering Cancer Center, 1275 York Avenue, New York, NY, 10065; e-mail: a-haimovitz-friedman@ski.mskcc.org.

survival factors for endothelium, such as vascular endothelial growth factor (VEGF), acidic and basic fibroblast growth factors (bFGFs) and interleukin 11 (IL-11), protect these target organs from radiation injury by affecting the same pathway (*14*). Our group and others have reported on work that demonstrated the relevance of this mechanism in radiation-induced damage to the gastrointestinal tract, lung and brain (*12, 15, 16*).

Current management approaches of SG hypofunction remain palliative and are generally unsatisfactory. Amifostine (WR-2721; 2-[(3-aminopropyl) amino] ethylphosphorothioic acid) has been recently approved for prevention of xerostomia in HNSCC patients undergoing radiotherapy, however, there is still controversy as to whether Amifostine also confers tumor protection (*17*). The goal of this study was to elucidate the mechanism by which radiation affects SG microvasculature and causes SG hypofunction. Our study demonstrates that radiation-induced SG hypofunction is mediated via endothelial apoptosis and microvascular dysfunction involving ceramide and reactive oxygen species (ROS) generation.

MATERIALS AND METHODS

Cell Culture and Irradiation

Bovine aortic endothelial cells (BAECs) were grown to confluence in DMEM (Thermo Fisher Scientific, Waltham, MA), supplemented with glucose (1 g/l), 10% heat-inactivated bovine calf serum, penicillin (50 units/ml) and streptomycin (50 μg/ml). Human recombinant bFGF (R&D Systems™, Minneapolis, MN) was added every other day during the phase of exponential growth. Prior to irradiation the cultures were washed and serum-free media was added. Cells were gamma irradiated on ice with single doses between 0 and 15 Gy using the Shepherd Mark I irradiator with a Cesium-137 source (San Fernando, CA) at a rate of 2.08 Gy/min. For experiments involving incubations of under 10 min, cells were irradiated on ice and thereafter warmed in a 37°C water bath for the indicated times. In the control experiments the cells were sham irradiated. Immediately after irradiation the cells were incubated at 37°C.

4-Hydroxy-2, 2,6,6-tetramethylpiperidine-*N*-oxyl (Tempol) (Sigma-Aldrich® LLC, Milwaukee, WI) and *N*-acetyl cysteine (NAC) (Sigma-Aldrich) were added 10 min prior to irradiation and removed 1 h later.

Ceramide Quantification

Ceramide was quantified by the diacylglycerol kinase assay as described previously (*9*). At indicated time points after irradiation cells were washed twice with ice cold phosphate buffered saline (PBS), and extracted with chloroform: methanol: 1 *N* HCI (100:100:1, v/v/v). Lipids in the organic phase extract were dried under N_2 and subjected to mild alkaline hydrolysis (0.1 *N* methanolic KOH for 1 h at 37°C) to remove glycerophospholipid. Samples were reextracted, and the organic phase was dried under N_2. Ceramide contained in each sample was resuspended in a 100 μl reaction mixture containing 150 μg of cardiolipin (Avanti® Polar Lipids Inc., Alabaster, AL), 280 μ*M* diethylenetriaminepentaacetic acid (DTPA, Sigma-Aldrich), 51 m*M* octyl-β-D-glucopyranoside (Calbiochem, Golden, CO), 50 m*M* NaCl, 51 m*M* imidazole, 1 m*M* EDTA, 12.5 m*M* $MgCl_2$, 2 m*M* dithiothreitol (DTT), 0.7% glycerol, 70 μ*M* β-mercaptoethanol, 1 m*M* ATP, 10 μCi of [gamma-^{32}P] ATP (300 Ci/mmol; Amersham International plc, Little Chalfont, UK), 35 μg/ml *Escherichia coli* diacylglycerol kinase (Calbiochem, Golden, CO) at pH 6.5. After 30 min at room temperature, the reaction was stopped by extraction of lipids with 1 ml of chloroform: 1 *N* HCI (100:100:1, v/v/v), 170 μl buffered saline solution (BSS; 135 m*M* NaCl, 1.5 m*M* $CaCI_2$, 0.5 m*M* $MgCl_2$, 5.6 m*M* glucose and 10 m*M* HEPES, pH 7.2) and 30 μl of 100 m*M* EDTA. The lower organic phase was dried under N_2. Ceramide-1-phoshate was resolved by thin-layer chromatography on silica gel 60 plates (Whatman/GE Healthcare, Maidstone, UK) using a solvent system of chloroform:methanol:acetic acid (65:15:5, v/v/v) and detected by autoradiography. Incorporated ^{32}P was quantified using a Fujix BAS 2000 TR phosphoimager.

Quantification of Apoptosis

Morphological nuclear changes typical for apoptosis were detected by staining with the DNA-binding fluorochrome *bis*-Benzamide (Hoechst 33258) (Sigma-Aldrich) as previously described (*9*). In short, cells were washed once with PBS and resuspended in 50 μl of 4% paraformaldehyde in PBS. After 10 min at room temperature, the fixative was removed and cells were washed once in PBS and resuspended in 15 μl of PBS containing 16 μg/ml *bis*-Benzamide. After 15 min incubation at room temperature, a 10 μl aliquot was placed on a glass slide, and 500 cells per slide were scored in duplicate for the incidence of apoptotic nuclear changes under an Olympus AH2-RFL fluorescence microscope with UGI exciter filter.

Animal Studies

Female C3H mice were purchased from Jackson Laboratories (Farmington, CT) were used for this study. Mice were used when they were 7–9 weeks old and weighed between 16–20 grams. All experiments were performed under the aegis of a protocol approved by the MSKCC Institute Animal Care and Use Committee (IACUC), and were in compliance with the Guide for the Care and Use of Laboratory Animal Resource, National Research Council.

In Vivo Irradiation

Irradiation of SGs was performed by placing each animal into a custom-made Lucite jig in such way that the animal could be immobilized without the use of anesthetics. Additionally, the jig was fitted with a Lucite cone that surrounded the head and prevented head movement during irradiation. Single 15 Gy doses were delivered to the head only by a Therapax DXT300 X-ray irradiator (Pantak Inc., East Haven, CT) using 2.0 mm aluminum filtration (300 KVp) at a dose rate of 1.9 Gy/min. This dose led to a significant (60%) loss of salivary flow in previously reported studies (*18*). To evaluate the radioprotective effect of ROS scavengers, 275 mg/kg of Tempol was injected intraperitoneally (ip) 10 min prior to irradiation to one of the groups (N = 5). Immediately after exposure, animals were removed from the Lucite jig and housed (5 animals/cage) in a climate- and light-controlled environment and allowed free access to food and water.

Evaluation of Acute Effects of Radiation on SG Microvasculature

To evaluate the acute effect of radiation on SG microvasculature mice were 15 Gy irradiated with or without Tempol pretreatment as described above and SGs were collected 4 h postirradiation. Microvessel density was calculated based on anti-CD31 staining. Endothelial apoptosis was determined by double immunostaining of SGs using anti-CD31 antibodies to detect the endothelial cells and anti-cleaved caspase-3 antibodies for the apoptotic cells and compared across the different treatment groups.

Evaluation of Long-Term Effects of Radiation on SGs

Saliva sample collection. To determine salivary flow rate, saliva samples were collected 8 weeks postirradiation. Mice were weighed and light anesthesia was induced with a solution of ketamine (100 mg/ml; Fort Dodge Animal Health, Fort Dodge, Iowa), xylazine (20 mg/ml; Phoenix Pharmaceutical Inc., St. Joseph, MO) in sterile water,

given ip (1 μl/1 mg of body weight). Saliva secretion was stimulated by subcutaneous (s.c.) injection of pilocarpine solution, 1 μl/g body weight (50 mg/ml). Saliva collection began within 2 min of pilocarpine administration. Animals were positioned with a 75 mm hematocrit tube (Drummond Scientific Co., Broomall, PA) placed in the oral cavity and whole saliva was collected in pre-weighed 0.75 ml Eppendorf tubes for 10 min. The amount of saliva collected was determined gravimetrically. Immediately afterwards, anesthetized animals were euthanized by cervical dislocation.

Saliva lysozyme levels using enzyme-linked immunosorbent assay (ELISA). To evaluate the quality of saliva, represented by lysozyme, a crucial enzyme for salivary functionality, lysozyme levels were measured in saliva samples collected from the mice 8 weeks postirradiation. Samples were kept in −80°C until analysis. A mouse lysozyme ELISA kit (LifeSpan BioSciences Inc., Seattle, WA) was used and the assay was done in triplicates. Lysozyme concentration was calculated using a fluorescent plate reader and determined after subtracting the background reading.

Immunofluorescence microvessel density assay. Submandibular and parotid SGs were collected from each mouse at the end of the experiment. Specimens were fixed with 4% paraformaldehyde, embedded in paraffin and sectioned to 5 μ sections for staining. Sections were stained with hematoxylin and eosin (H&E) or anti-CD31 and anti-cleaved caspase-3 antibodies. For microvessel density assay, SG sections stained with anti-CD31 antibodies were used, having 12 samples per group. The ImageJ processing program (NIH) (*4*), was used to calculate the number of vessels per gland and compare between groups.

Statistical Analysis

Analyses were performed using Stata Statistical Software (release 14.0; StataCorp LP, College Station, TX). Data are presented as mean ± standard deviation (SD). Analysis of variance (ANOVA) test was used to analyze differences among groups and Bonferonni correction method was used for multiple comparisons.

RESULTS

Radiation-Induced Apoptosis in Endothelial Cells is Mediated via ROS Generation

Previous studies have shown that Tempol protected C3H mice from SG hypofunction induced by single high-dose radiation (15–17.5 Gy) (*19, 20*). These results indicate that ROS (*21*) might be involved in the radiation effect on the SGs. In addition, protection against loss of endothelial cells through localized administration of angiogenic factors rescued the endothelial cell from radiation-induced apoptosis, prevented radiation-induced damage to the microvasculature of the SGs and improved SG hypofunction after irradiation, thus diminishing morbidity of the mice (*8*). Therefore, we decided to evaluate the role of ROS in radiation-induced, ceramide-mediated apoptosis *in vitro* and used two well-established free radical scavengers. Tempol, a stable nonspecific free radical scavenger and NAC, thiol antioxidant and glutathione precursors were added 10 min prior to irradiation. Both Tempol (5 m*M*) and NAC (50 m*M*) significantly inhibited radiation-induced apoptosis at 8 h by 71% and 60%, respectively ($P > 0.005$; Fig. 1A). In parallel, we treated the BAECs with 1 m*M* hydrogen peroxide (H_2O_2). At this concentration H_2O_2 induced 60% apoptosis in BAECs at 24 h and both Tempol (5 m*M*) and NAC (50 m*M*) completely abolished H_2O_2-induced apoptosis in these cells, demonstrating the effectiveness of Tempol and NAC at the concentrations used to serve as ROS scavenger in these cells (data not shown).

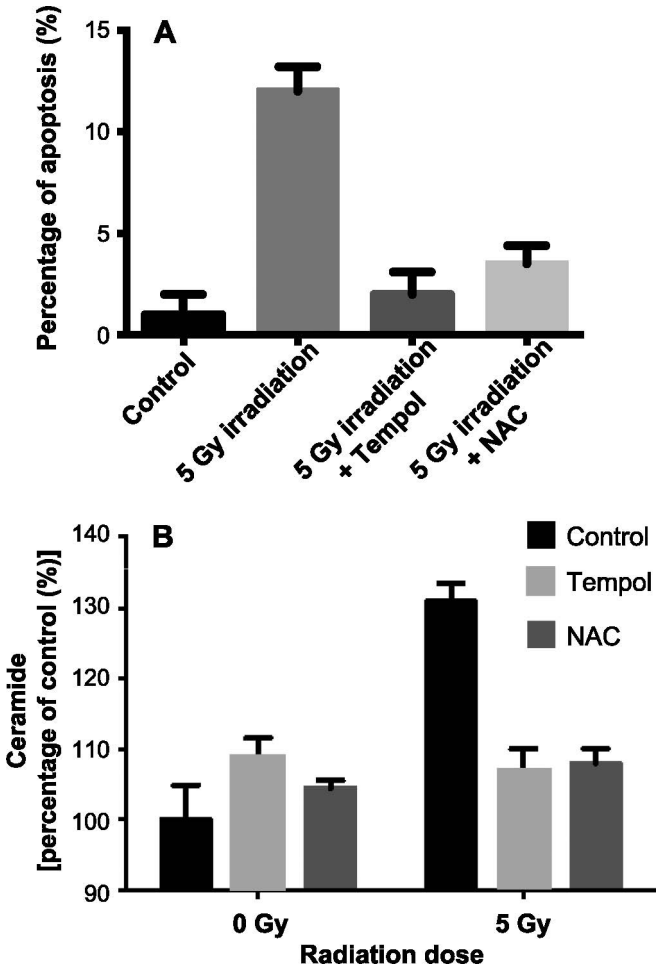

FIG. 1. Free radical scavengers inhibit radiation-induced apoptosis and ceramide generation in bovine aortic endothelial cells (BAECs). Tempol or NAC was added to BAECs 10 min prior to 5 Gy irradiation (5 m*M* and 50 m*M*, respectively). Panel A: Apoptosis was scored 8 h after irradiation using the *bis*-Benzamide trihydrochloride staining. Panel B: Ceramide levels were measured using the diacylglycerol kinase assay 15 min after 5 Gy irradiation. Data are expressed as mean ± SD from three independent experiments.

Since it has been suggested that ROS cause membrane lipid peroxidation and may function as second messengers in receptor-mediated signal transduction, we tested the effect of Tempol and NAC on radiation-induced ceramide formation in BAECs. Figure 1B shows an increase of more than 30% in cellular ceramide levels at 15 min after 5 Gy compared to controls ($P < 0.005$). These results are similar to data previously obtained in these cells, and are sufficient to initiate an apoptotic response in the BAECs. Pre-incubation of the BAECs with either Tempol or NAC prevented this radiation-induced increase in ceramide, suggesting that ceramide generation is dependent on ROS

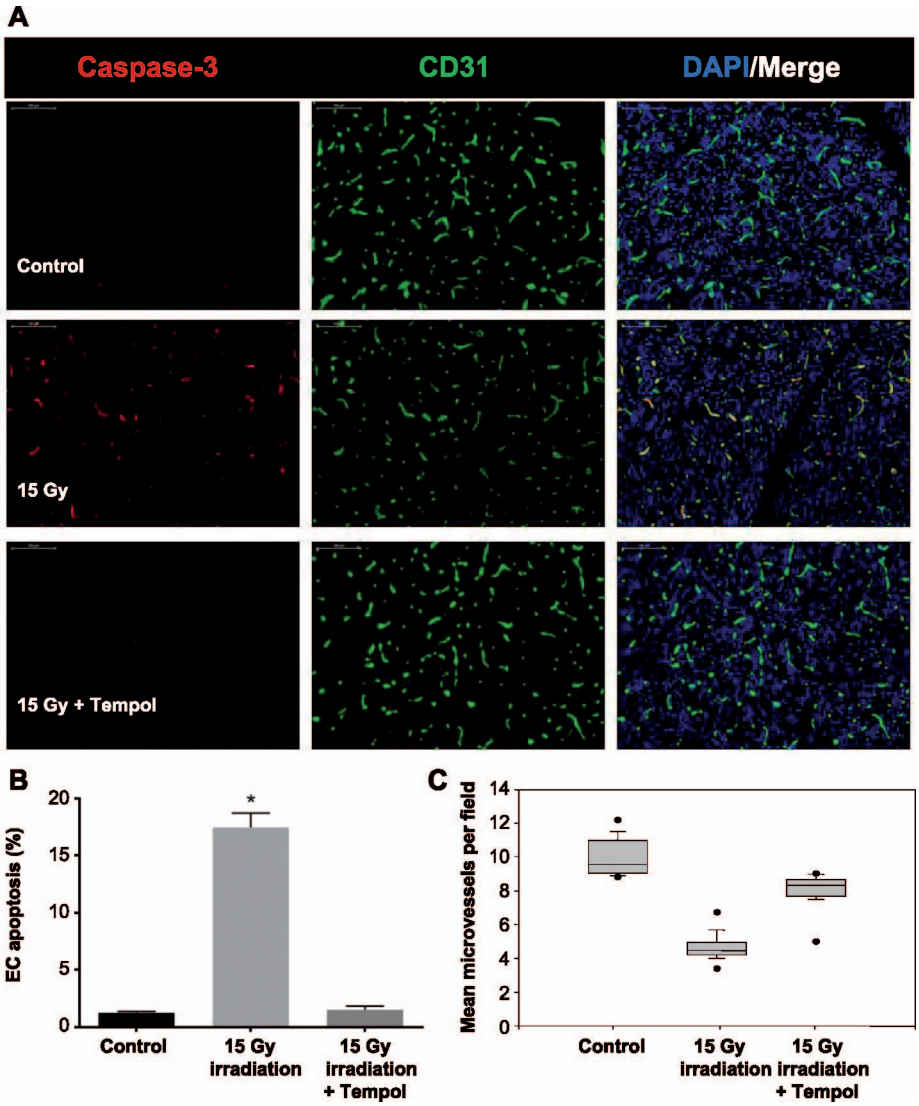

FIG. 2. Irradiation of the salivary glands results in endothelial cell apoptosis and a decrease in microvessel density (MVD) attenuated by treatment with Tempol during irradiation. Panel A: Immunofluorescence staining of mouse SGs 4 h after 15 Gy irradiation of the head and neck region. SGs were stained with anti-CD31 and anti-cleaved caspase-3 antibodies. Panel B: Quantification of apoptosis in the microvasculature of the SG at 4 h postirradiation (shown in panel A). $^{**}P < 0.001$. Panel C: The average number of $CD31^+$ endothelial cells in the control and Tempol-treated groups was significantly higher compared to the radiation only treatment group 4 h after exposure. $CD31^+$ cells in SGs with 95% CIs are shown in a box plot. The upper boundary of the box represents the 75th percentile of the number of double positive per field per mouse. The lower boundary of the box represents the 25th percentile of the data distribution. The horizontal line within the box represents the median value and the error bars represent the 95% CIs. The closed circles above and below the bars represent out-of-range values. A total of 12 glands from six mice in each treatment group were studied, and 40 fields per gland were counted.

formation. Treatment of BAECs with Tempol or NAC alone had no significant effect on ceramide levels in these cells.

Acute Effects of Radiation on SG Microvasculature

It has been previously shown that 15 Gy irradiation induced a 60% reduction in the salivary flow rate, which was significantly protected by Tempol pretreatment (*19, 20*). Here we show that 15 Gy irradiation induced 17.4% ± 2.1% apoptosis 4 h after treatment within the SGs of C3H mice (Fig. 2A and B) and this effect was completely inhibited if mice were pretreated with Tempol. Whereas 15 Gy irradiation induced a 50% reduction in microvascular density (MVD) within the SG of C3H mice, pretreatment with Tempol significantly protected the endothelial cells and the MVD within the SGs dropped only by 10.5% compared to the control group (Fig. 2C). These results indicate that radiation-induced microvascular dysfunction resulting in decreased MVD within the SG is ROS mediated and Tempol can serve as a radioprotector of the endothelial cells, thus restoring the salivary flow rate.

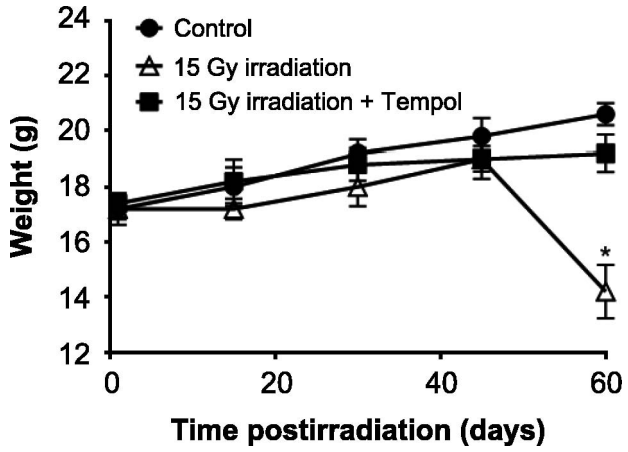

FIG. 3. Irradiation (15 Gy) to the head and neck region results in significant weight loss ameliorated by Tempol. Average body weight of mice during 8 weeks after treatment with 0 or 15 Gy radiation only or 15 Gy radiation with Tempol 275 mg/kg (N = 5 mice per group). *$P < 0.05$.

Long-Term Effects of Radiation on SG Microvasculature

We tested the effect of radiation on SG function. By eight weeks postirradiation all the mice in the radiation only group had lost 30% of their body weight, developed severe hair loss on their scalp and were in poor general condition (Fig. 3). The irradiated mice pretreated with Tempol did not develop these conditions and looked almost identical to the control group.

While no apparent gross histological differences were observed between the irradiated and nonirradiated SGs, microvessel density within the SGs was significantly lower in the radiation only group compared to the SGs from the control group ($P < 0.01$). This effect was also ameliorated with administration of Tempol prior to irradiation ($P < 0.05$, Fig. 4A and B).

Mice in the radiation only group also developed salivary hypofunction manifested by significantly reduced saliva production compared to nonirradiated mice ($P < 0.001$). This effect was partially reversed by pretreatment with Tempol ($P < 0.05$). The mice in the control group showed a mean salivary flow of 692 ± 48 µl/10 min, while the radiation only group had a mean salivary output of 195 ± 12 µl/10 min and the radiation with Tempol group had 265 ± 28 µl/10 min (Fig. 5A). As for saliva quality, lysozyme levels were significantly decreased 8 weeks postirradiation compared to the control group ($P < 0.05$). However, this effect was not prevented by Tempol pretreatment (Fig. 5B).

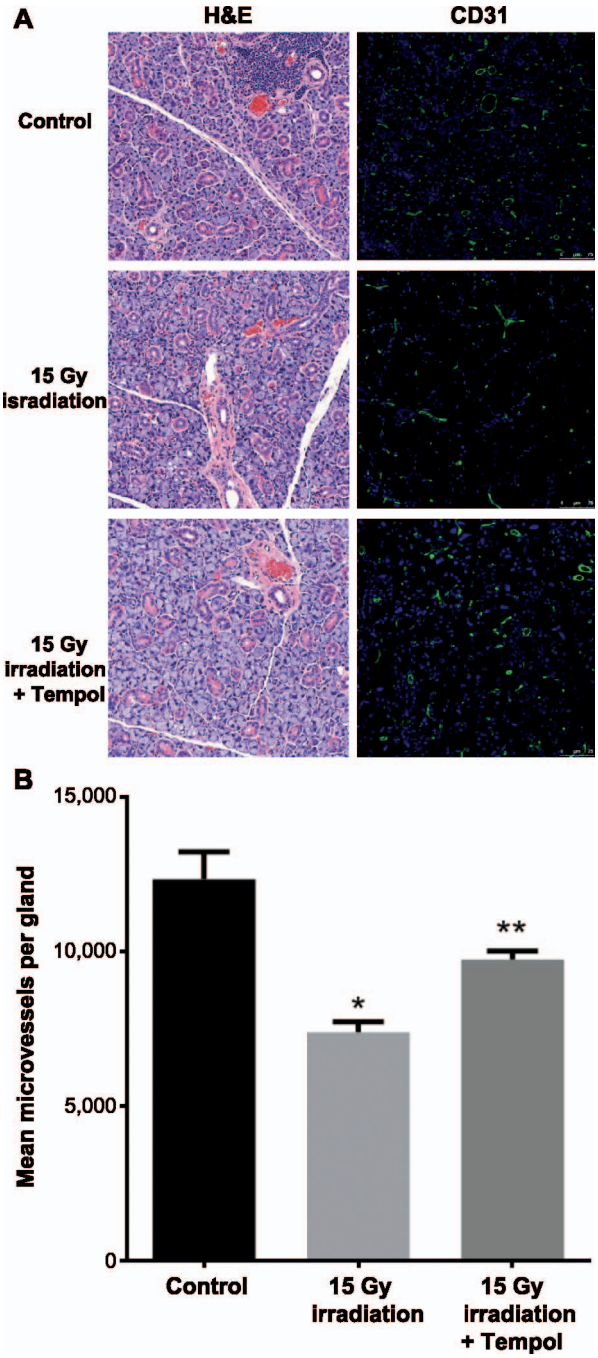

FIG. 4. Tempol ameliorates late effects of ionizing radiation in mouse SGs. Panel A: Representative H&E and immunofluorescent staining with anti-CD31 antibody of mouse SG 8 weeks after treatment with 0 or 15 Gy radiation only or 15 Gy radiation with Tempol 275 mg/kg. Panel B: Irradiation with 15 Gy causes significant decrease in MVD 8 weeks after treatment. MVD in salivary glands was calculated as the number of $CD31^+$ area per gland from four different sections per mouse (N = 5 mice per group). *,**$P < 0.05$. Tempol significantly ameliorated this effect.

DISCUSSION

In the current study we investigated the effect of radiation-induced microvascular damage via activation of the ASMase pathway and generation of ROS on SG function. First, we have shown that ROS scavengers inhibited both ceramide generation and endothelial cell apoptosis, indicating that in these cells radiation-induced ceramide-mediated endothelial apoptosis is ROS dependent. Second, we found that a single 15 Gy radiation dose causes clinical, biochemical and histological changes to the SGs in a murine model, similar to effects observed in patients

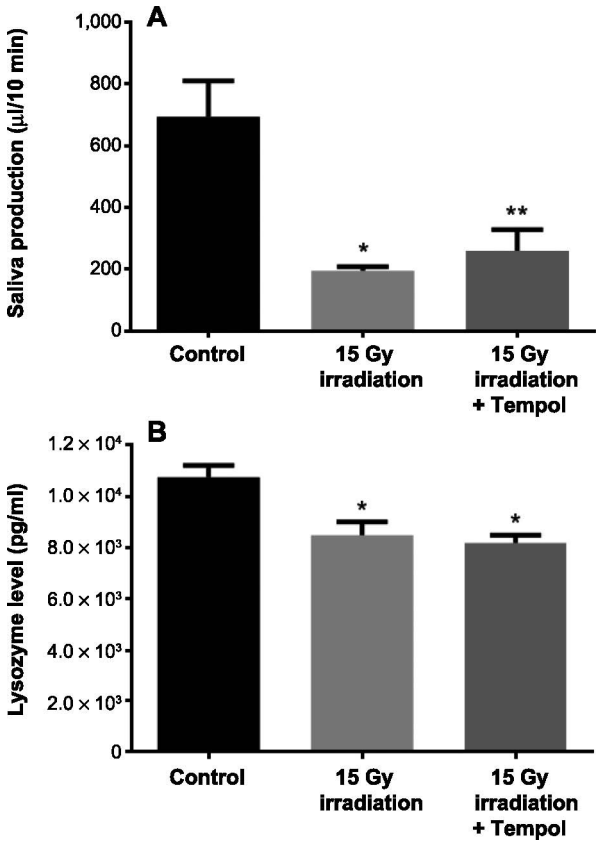

FIG. 5. Tempol reduces radiation-induced salivary gland hypofunction. Panel A: Average saliva production collected during 10 min after s.c. administration of pilocarpine 50 mg/kg in mice 8 weeks after treatment with 0 or 15 Gy radiation only or 15 Gy radiation with Tempol 275 mg/kg (N = 5 mice per group). *$P < 0.05$; **$P < 0.001$. Panel B: Average saliva lysozyme concentration measured in mouse saliva 8 weeks after treatment with 0 or 15 Gy radiation only or 15 Gy radiation with Tempol 275 mg/kg using ELISA assay (N = 5 mice per group). *$P < 0.05$.

undergoing radiotherapy. Moreover, we were able to demonstrate the protective effect of ROS scavengers on salivary microvasculature by ''shutting down'' the process that was initialized by irradiation. This protective effect reduced both acute and chronic microvascular damage in the SGs and as a consequence, prevented clinically significant salivary hypofunction. However, the effect of radiation on saliva quality manifested by significantly reduced lysozyme levels has not been attenuated by ROS scavenging and microvessel protection, suggesting the involvement of an additional/different mechanism (*22*).

In previous studies, it has been reported that activation of the ASMase signal transduction pathway by irradiation leads to endothelial dysfunction manifested by apoptosis, increased permeability and local inflammation (*14*). A recent study on microvascular endothelial cells in miniature pig parotid glands showed that a single radiation dose led to a significant reduction of microvessel density and local blood flow rate. The authors concluded that significant and rapid increase of ASMase activity levels might play an important role in radiation-induced salivary hypofunction (*7*). In another study, using the same animal model, the authors found that dose-volume distribution is an important factor in the radiobiology of SGs (*23*). As for acinar progenitor cells, previously reported studies suggest that these cells require a healthy microenvironment to differentiate to mature acinar cells and thus damage to the microvasculature could lead to long-term SG hypofunction (*18*). HNSCC is the sixth most common malignancy worldwide (*1*) and the curative treatment modalities consist of surgery and/or radiation therapy. Currently, one of the main challenges in treating HNSCC patients is in selectively protecting normal tissue without compromising the therapeutic effects of radiation. In a study that addressed this issue, Tempol provided SG radioprotection and did not interfere with the tumor response (*24*). These results are consistent with the hypothesis that differential radioprotection by Tempol resides in faster reduction to the non-radioprotective hydroxylamine in the tumor compared to normal tissues (*25, 26*). Further development of ROS scavengers and thiol antioxidants is warranted for human clinical trials as a selective protector against radiation-induced SG damage (*27*).

Li *et al.* (*28*) described a mechanism for microvascular dysfunction by activation of the ASMase/ceramide pathway. According to that mechanism, in response to various stimuli, membrane lipid rafts are clustered to aggregate or recruit NADPH oxidase subunits and related proteins in vascular endothelial cells, forming redox-signaling platforms (*28*). We propose that radiation exposure can induce ASMase activation, which triggers the generation of ceramide-rich macrodomains (CRMs), NADPH oxidase activation and subsequent production of ROS (*21*), resulting in microvascular dysfunction. We have previously shown that radiation induces CRMs in endothelial cells (*16*). Endothelial cells are 20-fold enriched in secretory ASMase compared to any other cell in the body, and are particularly sensitive to radiation-induced apoptosis *in vitro* and *in vivo* (*11*). Our previous studies have shown that endothelial apoptosis and microvascular dysfunction after single high-dose irradiation contribute significantly to tumor cell lethality and tumor cure but also to normal tissue toxicity (*21*). A major mechanism by which NOX-derived ROS contribute to vascular damage is via superoxide ($O_2^{\bullet -}$)-mediated inactivation of NO, leading to a loss of its vasoprotective actions and the formation of peroxynitrite ($ONOO^-$). Peroxynitrite is a powerful oxidant that causes irreversible damage to macromolecules, including proteins, lipids and DNA, thereby disrupting crucial cell signaling pathways and promoting cell death (*29*). In addition, ROS can activate ASMase, thus perpetuating the oxidative stress environment for a period that exceeds the capacity of the acinar progenitor cells to differentiate into mature acinar cells, leading to the long-term SG hypofunction observed in response to radiation.

In summary, this study demonstrates that single-dose irradiation leads to changes in microvascular endothelial

cells within the SGs, mediated by ceramide and ROS generation, which affect SG function. Furthermore, we showed that ROS scavengers were able to prevent radiation-induced microvascular damage and SG hypofunction, suggesting a possible therapeutic approach for these compounds.

ACKNOWLEDGMENTS

We thank Karen Reede for assistance in preparation of the manuscript and Evan Darling from the Molecular Cytology Facility for his help with the IF apoptotic staining. This study was supported in part through the NIH/NCI Cancer Center Support Core Grant (no. P30 CA008748), and by the Department of Radiation Oncology, Memorial Sloan Kettering Cancer Center.

Received: February 22, 2016; accepted: June 8, 2016; published online: July 26, 2016

REFERENCES

1. Siegel RL, Miller KD, Jemal A. Cancer statistics, 2016. CA Cancer J Clin 2016; 66:7–30.
2. Bourhis J, Overgaard J, Audry H, Ang KK, Saunders M, Bernier J, et al. Hyperfractionated or accelerated radiotherapy in head and neck cancer: a meta-analysis. Lancet 2006; 368:843–54.
3. Pignon JP, le Maitre A, Maillard E, Bourhis J. Meta-analysis of chemotherapy in head and neck cancer (MACH-NC): an update on 93 randomised trials and 17,346 patients. Radiother Oncol 2009; 92:4–14.
4. Cox JD, Stetz J, Pajak TF. Toxicity criteria of the Radiation Therapy Oncology Group (RTOG) and the European Organization for Research and Treatment of Cancer (EORTC). Int J Radiat Oncol Biol Phys 1995; 31:1341–6.
5. Jensen SB, Pedersen AM, Vissink A, Andersen E, Brown CG, Davies AN, et al. A systematic review of salivary gland hypofunction and xerostomia induced by cancer therapies: management strategies and economic impact. Support Care Cancer 2010; 18:1061–79.
6. Nagler RM. The enigmatic mechanism of irradiation-induced damage to the major salivary glands. Oral Dis 2002; 8:141–6.
7. Xu J, Yan X, Gao R, Mao L, Cotrim AP, Zheng C, et al. Effect of irradiation on microvascular endothelial cells of parotid glands in the miniature pig. Int J Radiat Oncol Biol Phys 2010; 78:897–903.
8. Cotrim AP, Sowers A, Mitchell JB, Baum BJ. Prevention of irradiation-induced salivary hypofunction by microvessel protection in mouse salivary glands. Mol Ther 2007; 15:2101–6.
9. Haimovitz-Friedman A, Kan CC, Ehleiter D, Persaud RS, McLoughlin M, Fuks Z, et al. Ionizing radiation acts on cellular membranes to generate ceramide and initiate apoptosis. J Exp Med 1994; 180:525–35.
10. Kolesnick R, Fuks Z. Radiation and ceramide-induced apoptosis. Oncogene. 2003; 22:5897–906.
11. Haimovitz-Friedman A, Cordon-Cardo C, Bayoumy S, Garzotto M, McLoughlin M, Gallily R, et al. Lipopolysaccharide induces disseminated endothelial apoptosis requiring ceramide generation. J Exp Med 1997; 186:1831–41.
12. Fuks Z, Alfieri A, Haimovitz-Friedman A, Seddon A, Cordon-Cardo C. Intravenous basic fibroblast growth factor protects the lung but not mediastinal organs against radiation-induced apoptosis in vivo. Cancer J Sci Am 1995; 1:62–72.
13. Paris F, Fuks Z, Kang A, Capodieci P, Juan G, Ehleiter D, et al. Endothelial apoptosis as the primary lesion initiating intestinal radiation damage in mice. Science 2001; 293:293–7.
14. Li YQ, Chen P, Haimovitz-Friedman A, Reilly RM, Wong CS. Endothelial apoptosis initiates acute blood-brain barrier disruption after ionizing radiation. Cancer Res 2003; 63:5950–6.
15. Pena LA, Fuks Z, Kolesnick RN. Radiation-induced apoptosis of endothelial cells in the murine central nervous system: protection by fibroblast growth factor and sphingomyelinase deficiency. Cancer Res 2000; 60:321–7.
16. Rotolo J, Stancevic B, Zhang J, Hua G, Fuller J, Yin X, et al. Anti-ceramide antibody prevents the radiation gastrointestinal syndrome in mice. J Clin Invest 2012; 122:1786–90.
17. Nagler RM, Baum BJ. Prophylactic treatment reduces the severity of xerostomia following radiation therapy for oral cavity cancer. Arch Otolaryngol Head Neck Surg 2003; 129:247–50.
18. Konings AW, Coppes RP, Vissink A. On the mechanism of salivary gland radiosensitivity. Int J Radiat Oncol Biol Phys 2005; 62:1187–94.
19. Vitolo JM, Cotrim AP, Sowers AL, Russo A, Wellner RB, Pillemer SR, et al. The stable nitroxide tempol facilitates salivary gland protection during head and neck irradiation in a mouse model. Clin Cancer Res 2004; 10:1807–12.
20. Cotrim AP, Sowers AL, Lodde BM, Vitolo JM, Kingman A, Russo A, et al. Kinetics of tempol for prevention of xerostomia following head and neck irradiation in a mouse model. Clin Cancer Res 2005; 11:7564–8.
21. Garcia-Barros M, Paris F, Cordon-Cardo C, Lyden D, Rafii S, Haimovitz-Friedman A, et al. Tumor response to radiotherapy regulated by endothelial cell apoptosis. Science. 2003; 300:1155–9.
22. Laheij AM, Rasch CN, Brandt BW, de Soet JJ, Schipper RG, Loof A, et al. Proteins and peptides in parotid saliva of irradiated patients compared to that of healthy controls using SELDI-TOF-MS. BMC Res Notes 2015; 8:639.
23. Yan X, Hai B, Shan ZC, Zheng CY, Zhang CM, Wang SL. Effect of same-dose single or dual field irradiation on damage to miniature pig parotid glands. Int J Oral Sci 2009; 1:16–25.
24. Cotrim AP, Hyodo F, Matsumoto K, Sowers AL, Cook JA, Baum BJ, et al. Differential radiation protection of salivary glands versus tumor by Tempol with accompanying tissue assessment of Tempol by magnetic resonance imaging. Clin Cancer Res 2007; 13:4928–33.
25. Hahn SM, Sullivan FJ, DeLuca AM, Krishna CM, Wersto N, Venzon D, et al. Evaluation of tempol radioprotection in a murine tumor model. Free Radic Biol Med 1997; 22:1211–6.
26. Mitchell JB, DeGraff W, Kaufman D, Krishna MC, Samuni A, Finkelstein E, et al. Inhibition of oxygen-dependent radiation-induced damage by the nitroxide superoxide dismutase mimic, tempol. Arch Biochem Biophys 1991; 289:62–70.
27. Grdina DJ, Murley JS, Kataoka Y. Radioprotectants: current status and new directions. Oncology 2002; 63 Suppl 2:2–10.
28. Li PL, Zhang Y, Yi F. Lipid raft redox signaling platforms in endothelial dysfunction. Antioxid Redox Signal 2007; 9:1457–70.
29. Yi F, Jin S, Li PL. Lipid raft-redox signaling platforms in plasma membrane. Methods Mol Biol 2009; 580:93–107.